New microscopic indicators for evaluating traffic efficiency and safety

Transportation Research Interdisciplinary Perspectives 33 (2025) 101569

Contents lists available at ScienceDirect

Transportation Research Interdisciplinary Perspectives

journal homepage: www.elsevier.com/locate/trip

New microscopic indicators for evaluating traffic efficiency and safety

Eleonora Andreotti [a,b,*], Selpi [a,c]

[a] Division of Vehicle Safety, Department of Mechanics and Maritime Sciences, Chalmers University of Technology, SE 41296, Gothenburg, Sweden
[b] Digital Commons Lab, Fondazione Bruno Kessler, 38123, Povo (TN), Italy
[c] Department of Computer Science and Engineering, Chalmers University of Technology and University of Gothenburg, SE 41296, Gothenburg, Sweden

ARTICLE INFO

Keywords:
Safety
Efficiency
Safety–Efficiency Index
Combined Index

ABSTRACT

Improving both safety and efficiency in traffic systems remains a central challenge, especially in the context of increasingly mixed traffic with autonomous and human-driven vehicles. Although many indicators assess either safety or efficiency, few capture both dimensions simultaneously at a microscopic level. This paper introduces two new traffic indicators: *Efficiency Index* (EI), which measures local speed and spacing regularity, and *Safety and Efficiency Index* (SEI), which combines EI with a time-to-collision safety component. A tunable version, *SEMI*, allows greater sensitivity to risk by penalizing safety-critical interactions. Using real-world traffic flow data and simulation via SUMO, we tested these indicators in varying penetration rates of autonomous vehicles. The results show that while AVs improve efficiency across the board, the safety gains become especially pronounced in dense traffic. These findings offer a flexible and interpretable tool for researchers and practitioners in traffic engineering, vehicle automation, and public policy. The proposed indicators can inform the design of AV control models, traffic management strategies, and infrastructure planning where safety-efficiency trade-offs must be explicitly addressed.

1. Introduction

More than 90% of traffic accidents are caused by human error (Singh, 2015). Autonomous vehicles (AVs), by replacing human drivers with intelligent systems, hold the promise of improving both safety and efficiency in traffic systems. Several studies suggest that AVs can reduce crash frequency (Arvin et al., 2021; Guériau and Dusparic, 2020; Virdi et al., 2019; Morando et al., 2018; Andreotti et al., 2020, 2022b,a), reduce travel times (Li et al., 2013; Kato et al., 2023), increase road capacity (Mahdavian et al., 2019; Sala and Soriguera, 2021), and improve flow stability (Parsa et al., 2020; Luo et al., 2024). However, due to limited access to real-world data, the impact of AVs is typically assessed through surrogate safety measures (SSMs) and microscopic simulation models.

Numerous SSMs have been proposed to assess traffic safety. Time-based indicators such as Time-To-Collision (TTC), Time-Exposed TTC (TET), Time-Integrated TTC (TIT) (Minderhoud and Bovy, 2001), and Modified TTC (MTTC) (Ozbay et al., 2008) are widely used. Time headway, the time gap between two vehicles at a fixed point (Michael et al., 2000), and Post-Encroachment Time (PET) (Cooper, 1984) also fall into this category. Other classes of indicators include deceleration-based metrics such as the Deceleration Rate to Avoid Collision (DRAC) and the Crash Potential Index (CPI), as well as distance-based indicators such as the Potential Index for Collision with Urgent Deceleration (PICUD) and the Proportion of Stopping Distance (PSD) (Allen et al., 1978). Comprehensive reviews can be found in Mahmud et al. (2017), Wang et al. (2021) and Hu et al. (2020).

Comparative studies have investigated how these measures perform in different traffic situations (Guido et al., 2011; Mamdoohi et al., 2014; Vogel, 2003). For example, TTC and PSD often identify overlapping risk scenarios (Mamdoohi et al., 2014), while TTC and time headway serve distinct purposes: TTC indicates imminent danger, while short time headways may signal potential risk or tailgating (Vogel, 2003). Most of these SSMs focus on rear-end collisions, though indicators have also been developed for lateral maneuvers such as cut-ins (Aramrattana et al., 2020; Andreotti et al., 2022a).

Although safety is typically analyzed using microscopic indicators, efficiency is typically assessed using macroscopic quantities such as average speed, density, and flow, through models such as the fundamental diagram (Imran et al., 2024), efficiency equations (Brilon, 2000), or congestion indices (He et al., 2016). However, to our knowledge, no single indicator combines safety and efficiency in a unified microscopic framework.

This gap is critical. Evaluating only safety or only efficiency can lead to skewed conclusions: enhancing one may compromise the other. As interest grows in minimizing emissions and optimizing infrastructure, combined indicators are increasingly necessary (Silva et al., 2022).

* Correspondence to: Fondazione Bruno Kessler (FBK), Via Sommarive 18, 38123, Povo (TN), Italy.
E-mail addresses: eandreotti@fbk.eu (E. Andreotti), selpi@chalmers.se (Selpi).

https://doi.org/10.1016/j.trip.2025.101569
Received 16 October 2024; Received in revised form 5 August 2025; Accepted 5 August 2025
Available online 19 August 2025

To address this, we propose two novel dimensionless indicators based on microscopic traffic data: *Efficiency Index* (EI), which quantifies the regularity and smoothness of vehicle interactions, and *Safety and Efficiency Index* (SEI), which integrates efficiency with a TTC-based safety component. Both indices range from 0 (unsafe and inefficient) to 1 (safe and efficient).

These indicators are designed to cover common traffic maneuvers (car-following, lane changing, and emergency braking) and are tested in realistic mixed traffic scenarios simulated in SUMO (Krajzewicz et al., 2012), incorporating real traffic flows and driver model calibration.

Although our approach is grounded in simulation-based analysis, it also addresses emerging challenges observed in real-world deployments of autonomous vehicles, particularly in complex mixed traffic environments that involve interactions with human-driven vehicles and vulnerable road users (Bjørnskau et al., 2023). The proposed indicators aim to support a broader understanding of AV integration by offering interpretable microscopic metrics that can inform both the modeling and evaluation frameworks.

In line with this interdisciplinary perspective, recent research has also investigated how shared autonomous micromobility modes can reshape travel behavior and system-level performance in dense urban contexts, reinforcing the relevance of integrated indicators that capture both safety and efficiency dimensions (Sánchez and Larson, 2024).

The remainder of the paper is organized as follows. Section 2 presents the formulation of the Efficiency Index (EI), while Section 3 introduces the Safety and Efficiency Index (SEI) and its modified version (SEMI). Section 4 illustrates their application through microsimulation of mixed traffic scenarios with varying levels of AV penetration. The key findings, implications, and future research directions are discussed in Sections 5 and 6.

2. Efficiency Index (EI)

To evaluate the efficiency of the car-following and lane change scenarios, we introduce *Efficiency Index* (EI). We define efficiency as vehicle behavior that promotes traffic flow stability, specifically scenarios where vehicles maintain similar speeds and consistent spacing. For example, platoon formation is considered highly efficient, whereas stop-and-go conditions are indicative of inefficiency.

The EI between two vehicles in a car-following situation is computed using two components: a parabolic function that peaks when the ego vehicle's speed matches that of the leader (Fig. 1), and a negative exponential function that peaks when the relative spacing between the ego and the leader is minimal (Fig. 2). Fig. 3 illustrates how the EI varies with the distance between vehicles and the speed of the ego vehicle.

The equation that defines the EI between the ego vehicle E and the lead vehicle L is given by:

$$EI_{EL} := \left(1 - \left(\frac{s_E}{s_L} - 1\right)^2\right) \exp^{-|k_{EL} - k_{FE}|} \tag{1}$$

where s_E and s_L are the speeds of the ego and lead vehicles, respectively; and k_{EL} and k_{FE} are the relative distances defined as $k_{EL} := \frac{d_{EL}}{d_{EL}+d_{FE}}$ and $k_{FE} := \frac{d_{FE}}{d_{EL}+d_{FE}}$. Here, d_{EL} is the distance between the lead and the ego vehicles and d_{FE} is the distance between the ego and the following vehicles.

We then define the index over an entire road section as the average of the indices between each pair of vehicles. Let n be the number of vehicles involved in car-following; the total Efficiency Index is defined as:

$$EI^{tot} := \frac{1}{n-2} \sum_{i=2}^{n-1} \left(1 - \left(\frac{s_i}{s_{i+1}} - 1\right)^2\right) \exp^{-\left|\frac{d_{i,i+1} - d_{i-1,i}}{d_{i,i+1} + d_{i-1,i}}\right|}. \tag{2}$$

Both indices take values between 0 and 1, where 0 represents the lowest efficiency and 1 the highest. We also note that the more similar

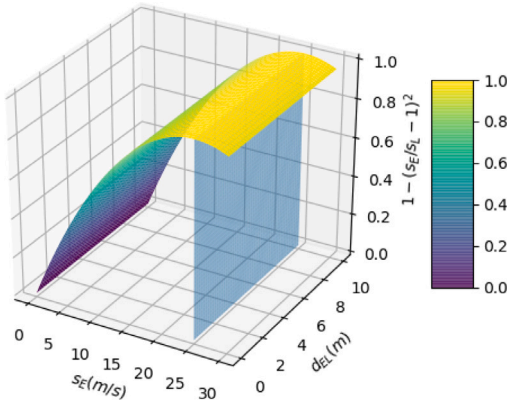

Fig. 1. Parabolic component of the Efficiency Index (EI) as a function of the distance between the ego vehicle and the leader vehicle (d_{EL}), and the speed of the ego vehicle (s_E). The blue plane represents the reference value given by the leader vehicle's speed (s_L), assuming a fixed distance of 10 m between the ego and the following vehicle (d_{FE}).

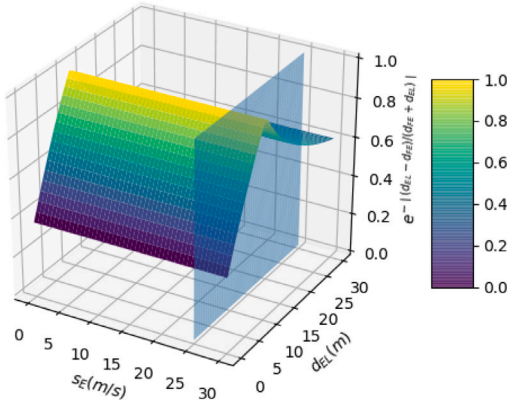

Fig. 2. Exponential component of the Efficiency Index (EI) as a function of the distance between the ego vehicle and the leader vehicle (d_{EL}), and the speed of the ego vehicle (s_E). The blue plane represents the reference value given by the leader vehicle's speed (s_L), assuming a fixed distance of 10 m between the ego and the following vehicle (d_{FE}).

the distances and speeds between vehicles, the higher the efficiency. Therefore, a platoon scenario will be rated as highly efficient by the EI, while a stop-and-go scenario will be rated as highly inefficient.

The total EI in (2) can be easily extended to include lane changes: When a vehicle is about to change lanes or is in the process of doing so, it is counted in both the starting and the target lanes. As shown in Fig. 4, when the vehicle E performs a lane change, it occupies both lanes; thus, we calculate both EI_{EL} and EI_{EA}. In a scenario with l lanes and n vehicles, of which m are changing lanes, the total EI consists of $(n-2l)+m$ terms, as given in (3).

In the particular case illustrated in Fig. 4, the total EI is defined as:

$$\begin{aligned} EI^{tot} &= \frac{1}{2}(EI_{EL} + EI_{EA}) \\ &= \frac{1}{2}\left(1 - \left(\frac{s_E}{s_L} - 1\right)^2\right) \exp^{-\left|\frac{d_{E,L} - d_{F,E}}{d_{E,L} + d_{F,E}}\right|} \\ &\quad + \frac{1}{2}\left(1 - \left(\frac{s_E}{s_A} - 1\right)^2\right) \exp^{-\left|\frac{d_{E,A} - d_{B,E}}{d_{E,A} + d_{B,E}}\right|}. \end{aligned} \tag{3}$$

3. Safety and Efficiency Index (SEI)

To define an index to evaluate safe and efficient car-following behavior, we consider driving patterns that are smooth, particularly

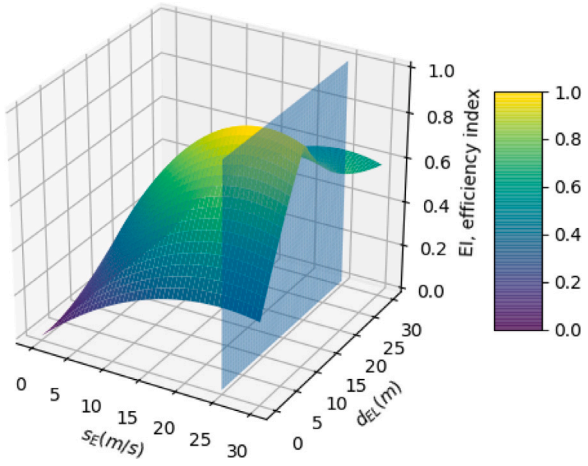

Fig. 3. Car-following Efficiency Index (EI) as a function of the ego vehicle's speed and its distance to the leader vehicle. The blue plane represents the leader vehicle's speed (s_L), assuming a fixed distance of 10 m between the ego and the following vehicle (d_{FE}).

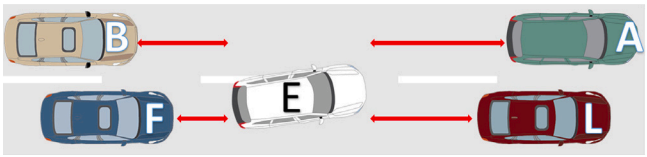

Fig. 4. The total EI extended to include lane changes.

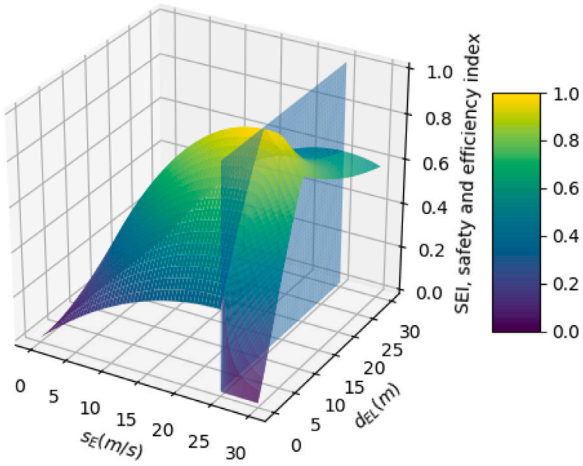

Fig. 5. Safety and Efficiency Index (SEI) as a function of the ego vehicle's speed and its distance to the leader vehicle. The blue plane represents the leader vehicle's speed (s_L), assuming a fixed distance of 10 m between the ego and the following vehicle (d_{FE}).

when in close proximity to other vehicles, and that promote traffic flow stability. Specifically, scenarios in which vehicles maintain similar speeds (within legal limits), maintain consistent spacing, and avoid abrupt acceleration or braking are considered safe and efficient. A platoon formation is considered highly efficient and safe, whereas stop-and-go conditions, especially those involving short headways and speed differences, are considered inefficient and unsafe.

To this end, we define *Safety and Efficiency Index* (SEI) as a combination of *Efficiency Index* (EI) and time-to-collision (TTC), as illustrated in Fig. 5.

The SEI between the ego vehicle E and the lead vehicle L is defined as follows:

$$SEI_{EL} := \begin{cases} EI_{EL}(1-\exp^{-TTC_{EL}}), & \text{if } s_E > s_L \\ EI_{EL}, & \text{otherwise} \end{cases} \tag{4}$$

where $TTC_{EL} = \frac{d_{EL}}{s_E - s_L}$, with $d_{EL} > 0$ and $s_E, s_L \leq s_{\max}$, where $s_{\max}$ is the speed limit of the road. The TTC is defined only when the speed of the ego vehicle exceeds that of the lead vehicle; otherwise, there is no risk of collision. According to this definition, when the leader's speed is greater than or equal to the speed of the ego vehicle, the SEI in Eq. (4) is based solely on efficiency (i.e., the EI in (1)). When the ego vehicle is faster than the leader, the SEI is computed as the EI penalized by the factor $(1-\exp^{-TTC})$.

For the reduction factor, we draw inspiration from the Cut-In Risk Indicator (CRI) (Aramrattana et al., 2020), as applied in Andreotti et al. (2022a). The CRI is defined as the sum of two exponential terms of the form $\exp^{-k\ TTC}$, which depend on the relative distances (k) and TTCs between the lead, ego, and following vehicles. Since we are not considering merging scenarios here, we replace the relative distance coefficients with the constant 1 and consider only the exponential term between the lead and ego vehicles. However, the SEI can be extended to merging situations using the reduction factor $(2-\exp^{-k_{EL}TTC_{EL}}-\exp^{-k_{FE}TTC_{FE}})$.

Like the EI, the SEI takes values between 0 and 1, where 0 indicates unsafe and inefficient conditions, and 1 indicates the safest and most efficient traffic state. We define the index over an entire road section as the average of the pairwise SEIs. Let n be the number of vehicles in car-following conditions; then the total SEI is given by:

$$SEI^{tot} := \frac{1}{n-2}\sum_{i=2}^{n-1} SEI_{i,i+1}. \tag{5}$$

If each lead vehicle is faster than its follower, that is, $s_i < s_{i+1}$ for all i, then SEI is equal to EI. As the ego vehicles become faster than their leaders and the distances between them decrease, the SEI decreases.

Consider a simple example involving three vehicles: L (leader), E (ego), and F (follower), with speeds and distances defined as in Section 2. Suppose that all inter-vehicle distances are 20 m, i.e. $d_{EL} = d_{FE} = 20$ m. If $s_L = 22$ m/s and $s_E = 20$ m/s, then TTC_{EL} is undefined and $EI_{EL} = SEI_{EL} = 0.9917$, indicating a highly efficient and safe scenario. If we slightly change the speeds to $s_L = 20$ m/s and $s_E = 22$ m/s, then $TTC_{EL} = 10$ s, and we get $EI_{EL} = 0.9900$ and $SEI_{EL} = 0.9899$.

As the speed difference increases, so does the gap between SEI and EI. For example: $s_L = 20$ m/s, $s_E = 25$ m/s $\rightarrow TTC = 4$ s, $EI_{EL} = 0.9375$,

Table 1
SEI, EI and TTC between E (ego) and L (leader) vehicles.

	$d_{FE} = 20$ m $d_{EL} = 20$ m	$d_{FE} = 21$ m $d_{EL} = 19$ m	$d_{FE} = 25$ m $d_{EL} = 15$ m
$s_E = 20$ m/s $s_L = 22$ m/s	EI = 0.9917 SEI = 0.9917	EI = 0.9434 SEI = 0.9434	EI = 0.7724 SEI = 0.7724
$s_E = 22$ m/s $s_L = 20$ m/s	EI = 0.9900 SEI = 0.9899 TTC = 10 s	EI = 0.9417 SEI = 0.9416 TTC = 9.5 s	EI = 0.7710 SEI = 0.7706 TTC = 7.5 s
$s_E = 25$ m/s $s_L = 20$ m/s	EI = 0.9375 SEI = 0.9203 TTC = 4.0 s	EI = 0.8918 SEI = 0.8718 TTC = 3.8 s	EI = 0.7301 SEI = 0.6938 TTC = 3.0 s
$s_E = 30$ m/s $s_L = 20$ m/s	EI = 0.7500 SEI = 0.6485 TTC = 2.0 s	EI = 0.7134 SEI = 0.6067 TTC = 1.9 s	EI = 0.5841 SEI = 0.4538 TTC = 1.5 s

$SEI_{EL} = 0.9203$; $s_L = 20$ m/s, $s_E = 30$ m/s $\rightarrow TTC = 2$ s, $EI_{EL} = 0.75$, $SEI_{EL} = 0.6484$.

In this example, where the distances are equal, the efficiency remains high, and thus SEI also remains relatively high. However, if we slightly modify the distances to $d_{EL} = 19$ m and $d_{FE} = 21$ m, the results become $EI_{EL} = 0.7134$ and $SEI_{EL} = 0.6067$. In a more critical case, with $d_{EL} = 15$ m, $d_{FE} = 25$ m, $s_L = 20$ m/s, and $s_E = 30$ m/s, the $TTC = 1.5$ s, a frequently cited critical threshold for rear-end risk (Meng and Qu, 2012), and SEI drops below 0.5, specifically at $SEI = 0.4538$. See Table 1 for more details.

From these examples, it becomes evident that we may sometimes wish to place greater emphasis on safety than on efficiency. To accommodate this, we introduce a penalty factor $\alpha \in (0, 1]$ that reduces the SEI value when the speed of the ego vehicle exceeds that of the lead vehicle. This leads to the definition of the *Safety and Efficiency Modified Index* (SEMI), given by:

$$SEMI_{EL} := \begin{cases} \alpha\ EI_{EL}(1 - \exp^{-TTC_{EL}}), & \text{if } s_E > s_L \\ EI_{EL}, & \text{otherwise} \end{cases} \tag{6}$$

where $TTC_{EL} = \frac{d_{EL}}{s_E - s_L}$, $d_{EL} > 0$, and $s_E, s_L \leq s_{\max}$, with $s_{\max}$ denoting the speed limit. The total SEMI is then defined as

$$SEMI^{tot} := \frac{1}{n-2} \sum_{i=2}^{n-1} SEMI_{i,i+1}. \tag{7}$$

When $\alpha = 1$, the SEMI formulation in Eq. (6) reduces to the SEI defined in Eq. (4), and remains continuous with respect to the speed difference between the ego and the lead vehicles. However, for any $\alpha < 1$, SEMI becomes a discontinuous function.

As shown in the previous example, even a modest penalty factor (for example $\alpha = 0.8$) leads to a substantial reduction in the SEI value, from its original value down to 0.3630, while the efficiency component remains unchanged.

These examples illustrate how SEMI can be effectively used to differentiate between traffic states that exhibit similar efficiency but varying safety levels. When safety is prioritized, the selection of a lower penalty factor ensures that the indicator attains high values only under very safe conditions, that is, when TTC-based conflicts are rare or TTC values are sufficiently large.

4. Case study: evaluation of EI and SEI in simulated mixed traffic conditions

To evaluate the proposed indices under different traffic scenarios, we reproduced a section of the DriveMe route in Gothenburg in SUMO. This segment consists of a 2-km long, three-lane main road and a 300-m on-ramp merging into it. The maximum speed allowed on the ramp is 80 km/h, while the speed limit on the main road is 90 km/h. Once the ramp joins the main road, there is a 200-m long acceleration lane.

Table 2
Parameters for HOCs and HOTs.

Parameter	HOCs	HOTs
model	krauss	krauss
length	norm(4.9, 0.2); [3.5, 5.5]	9.5
accel	norm(1.4976, 0.0555)	1.3
decel	norm(4.0522, 0.9979)	4
apparentDecel	decel	decel
sigma	norm(0.7954, 0.1615)	0.30
tau	gamma(33.62, 40.62)	2
minGap	norm(1.5401, 0.2188)	2.5
speedFactor	norm(1.2081, 0.1425)	1.17
lcStrategic	norm(0.0122, 1.6575)	0.7
lcCooperative	norm(0.9978, 0.1)	1.2
lcSpeedGain	1	0.75
lcKeepRight	1	1.9
lcAssertive	1.3	1
lcLookAheadLeft	2	2
lanechange-duration	1.1362	1.1362

Table 3
Parameters for AVs.

Parameter	Value
model	IDM
length	norm(4.9, 0.2); [3.5, 5.5]
accel	1.4
decel	2
delta	4
tau	1.5
minGap	2
speedFactor	1
lcStrategic	1
lcCooperative	1
lcSpeedGain	1
lcKeepRight	1
lcAssertive	1
lcLookAheadLeft	2
lanechange-duration	1.1362

Each simulation reproduces the real variation in traffic flow for a full day, specifically the 24-h period between 8 and 9 April 2019, based on data provided by the Swedish Transport Administration (Trafikverket) (Trafikverket, 2019). Since vehicle entry order and parameter values are generated stochastically, each simulation was run five times to ensure robustness. The Index values were calculated every minute, resulting in 300 evaluations per hour for both SEI^{tot} (5) and EI^{tot} (3). We evaluated the indicators separately for three segments of the road: the on-ramp, the main road before merging, and the main road after merging.

To realistically model Human-operated Cars (HOCs) and Human-operated Trucks (HOTs), we used the parameters calibrated for Gothenburg roads in Nilsson (2019) and Erlandson (2020), adopting the Krauss car-following model and a realistic lane change behavior (Table 2).

We modified baseline traffic by replacing increasing percentages of HOCs with Autonomous Vehicles (AVs) modeled using the Intelligent Driver Model (IDM), ranging from 0% to 100% in increments of 10%. AV parameters were taken from Kesting et al. (2010) and validated in Andreotti et al. (2020, 2022b) (Table 3).

4.1. Evaluation of EI

Table 4 and Fig. 8 present the average and boxplot of the total Efficiency Index (EI) for different penetration rates of AV during rush hours (i.e. average flow above 1 veh/s per road or 0.33 veh/s/lane).

4.1.1. Relationship between lane changes and AV penetration

To assess how lane changes impact efficiency, we computed their frequency as a function of AV penetration. The average number of lane changes per hour per km peaks at 0.1044 with 0% AVs and drops to

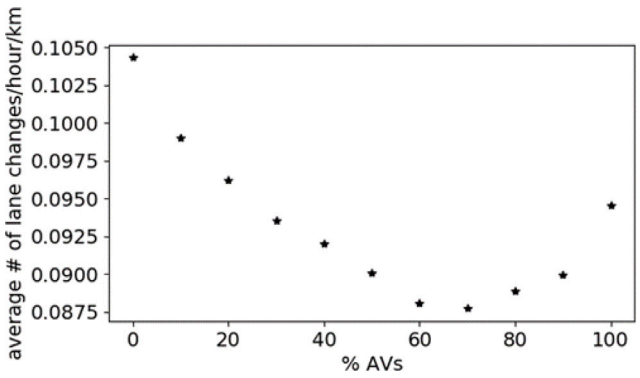

Fig. 6. Average number of lane changes/hour/km vs. AV penetration rate.

a minimum of 0.0877 at 70%, before rising again to 0.0945 at 100% AVs (Fig. 6). Although the standard deviations (not shown) are high, ranging from 0.0748 (0%) to 0.0591 (70%), the trend remains visible.

The frequency of lane changes varies considerably during the day. For 0% AVs, it ranges from 0.001 lane changes/hour/km (1–4 a.m.) to 0.22 (7–8 p.m.). Moreover, the daily trend changes with AV penetration; Fig. 7 shows representative time slots for selected rates. For example, with 100% AV, the number ranges from 0.002 (2–3 a.m.) to 0.17 (10–11 a.m.).

We observe that during rush hours, the higher penetration of AV is correlated with fewer lane changes. In contrast, during low-flow periods, the lane changes increase with AV penetration.

We tried to compare our results with naturalistic driving data (e.g. Li et al. (2015), based on Chinese highways). However, differences in traffic culture, driving styles, and the lack of information on flow variability make direct comparisons difficult. In addition, naturalistic data typically do not report how lane changes vary with density or traffic conditions.

In our simulations, average density was 13.6 veh/km, ranging from 0.77 veh/km (2–3 a.m.) to 44.1 veh/km (7–8 a.m.). The percentage of vehicles involved in lane changes ranged from 0.16% (3–4 a.m.) to 1.22% (11–12 p.m.) at 0% AVs. In particular, high density does not imply more lane changes: during rush hours (6–9 a.m.), lane changes dropped to around 0.5%, likely due to limited maneuverability. This aligns with more recent models (e.g. Knoop et al. (2012)), which consider both density and traffic dynamics, unlike earlier approaches that focused solely on density (Wardrop, 1952).

4.1.2. Efficiency across different AV penetration rates

As AV penetration increases, efficiency improves in both main road segments, except for a slight drop in 10% AVs. During rush hours, EI increases by up to 13.5% before the merging section and 19.8% after it. However, on the on-ramp, the trend is less consistent: efficiency decreases slightly at 10%–30% AVs (up to 3.5%) before increasing, reaching its peak at 100% AVs. In general, the on-ramp shows a more modest improvement, with a 9.3% increase between 0% and 100% AVs during peak hours (Table 4, Fig. 8).

Fig. 9 shows the average EI over time on the main road after merging, along with the total flow. In general, higher flow corresponds to higher EI, except for the 7–7:59 a.m. time slot, where EI slightly drops for AV rates higher than 50%, despite maximum flow. At nearly all hours, efficiency increases with penetration of AVs, except for 0% and 20% AVs, which yield nearly indistinguishable results, suggesting that a threshold above 20% may be necessary for AVs to positively impact efficiency.

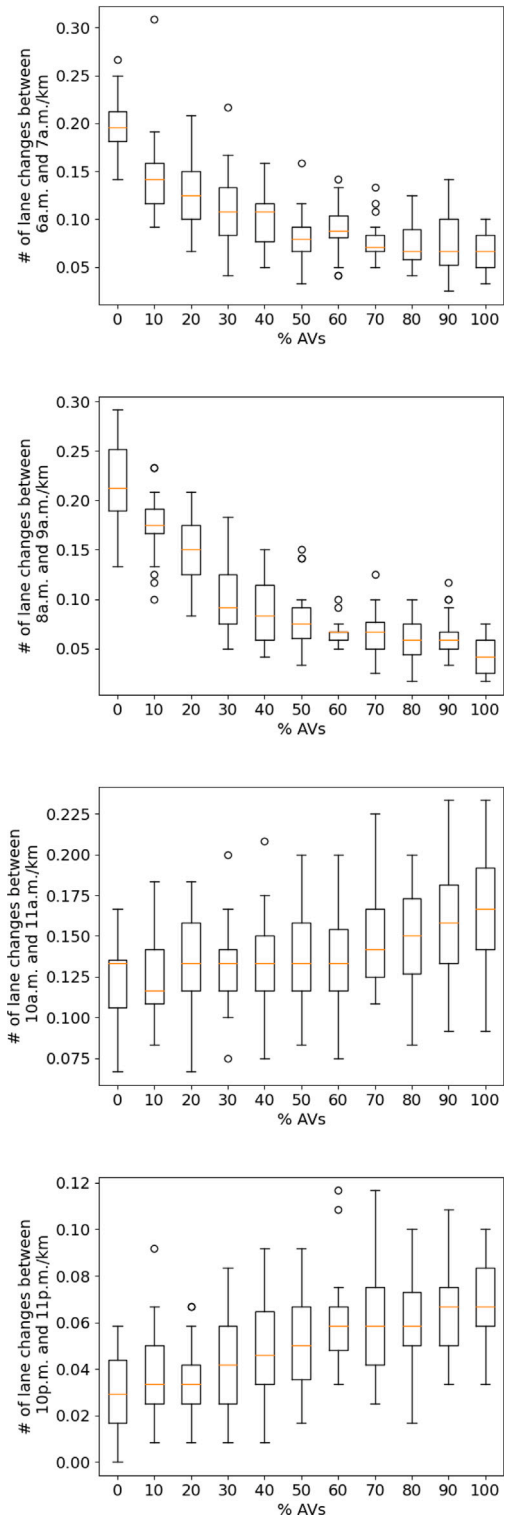

Fig. 7. Lane changes/hour/km vs. AV penetration and time of day.

4.1.3. Comparison of EI with the fundamental diagram

The fundamental diagram, also known as the flow–density relation, has traditionally been used to represent traffic efficiency, where higher flow implies higher efficiency (Daganzo et al., 2011; Daganzo and Geroliminis, 2008; Park et al., 2021; Lu et al., 2020). In some formulations, the flow is normalized by maximum capacity, yielding values between 0 and 1 (Othayoth and Rao, 2020; Frantzeskakis and Iordanis,

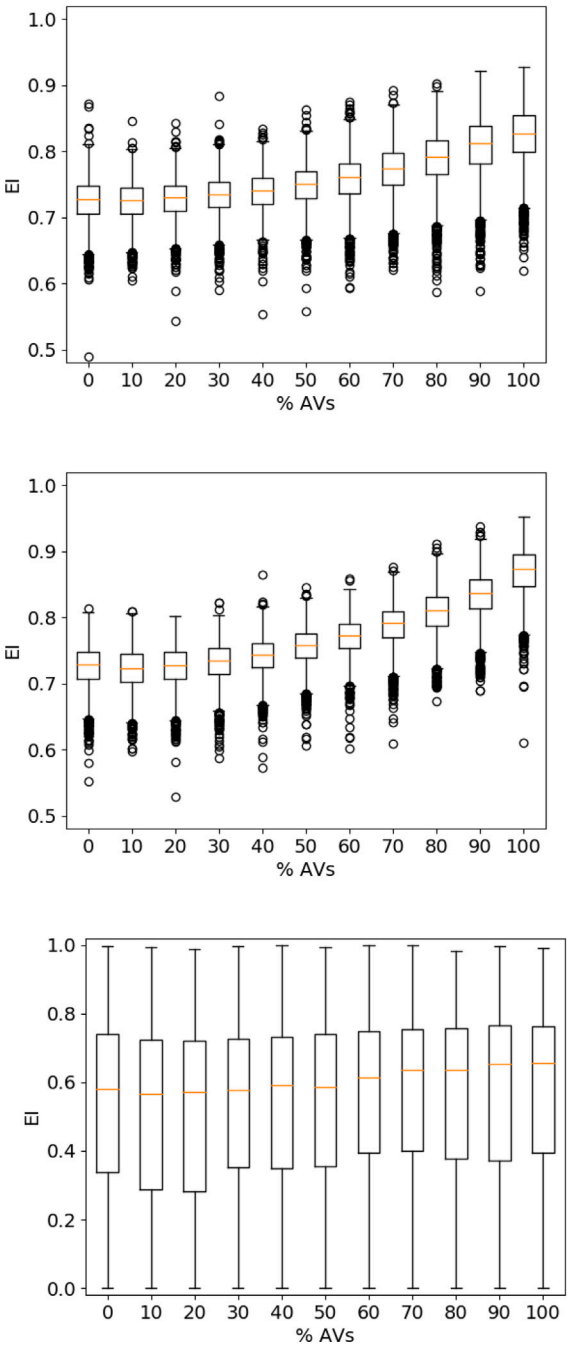

Fig. 8. EI values for different AV penetration rates during rush hours (6:00–8:59). From top to bottom: main road before merging, after merging, and on-ramp.

1987). Like the proposed EI, the fundamental diagram depends on the speeds and spacing of the vehicles. However, it reflects aggregate behavior by averaging these values (Daganzo and Geroliminis, 2008), while EI accounts for local variations among individual vehicles.

Fig. 10 illustrates how, under the same average speed and density, road conditions can differ significantly. In the top plot, speed variability across vehicles is introduced while keeping distances fixed: the curve with uniform speed (black) yields higher flow than curves with more heterogeneous speeds (lighter grays). In the bottom plot, inter-vehicle distances vary while speeds are held constant, again showing that variability reduces flow. Thus, even with identical mean values, local fluctuations in speed or distance can reduce overall efficiency, an effect captured by EI but not by standard fundamental diagrams.

Table 4
Mean total EI (3) values during rush hours for different AV penetration rates.

% AVs	Main road before merging	Main road after merging	On-ramp
0	0.7257	0.7256	0.5144
10	0.7242	0.7222	0.4965
20	0.7280	0.7256	0.4965
30	0.7339	0.7329	0.5118
40	0.7393	0.7413	0.5161
50	0.7484	0.7562	0.5215
60	0.7584	0.7706	0.5437
70	0.7720	0.7884	0.5498
80	0.7882	0.8080	0.5496
90	0.8069	0.8340	0.5552
100	0.8239	0.8695	0.5621

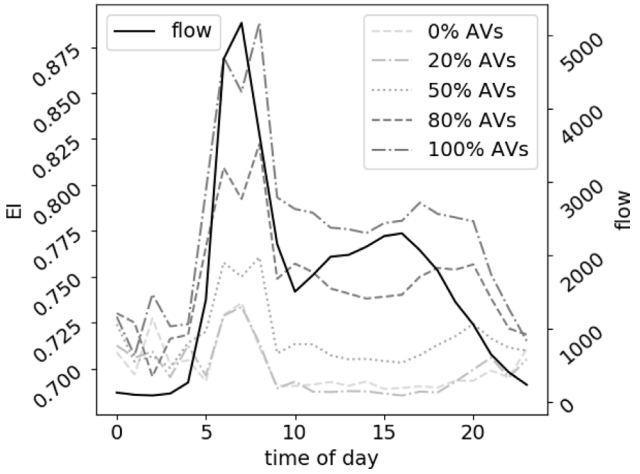

Fig. 9. Average EI for different AV penetration rates on the main road after merging, with corresponding traffic flow.

We used the Greenshield model (Greenshields, 1935) to generate the flow–density curves, although other models (e.g., Greenberg Pipes, 1967) could also be applied. The results confirm that at higher densities, variability in spacing or speed has a more pronounced impact on flow, further motivating the use of EI as a more granular efficiency metric.

4.2. Evaluation of SEI

We evaluated SEI under the same road conditions and time intervals used for EI. Table 5 reports the average total SEI values during rush hours for different penetration rates of AV. The values match closely those of EI, up to the fourth decimal place, except on the main road after merging, where SEI is slightly lower, probably due to higher flow levels increasing safety relevance. This similarity suggests that on Swedish roads, where traffic is relatively smooth, efficiency dominates SEI. However, to emphasize safety, we use the SEMI indicator (7), which penalizes SEI values when the ego vehicle exceeds the leader's speed. This is controlled by a factor $\alpha \in (0, 1]$, with lower values that emphasize safety more strongly.

Tables 6–8 show the SEMI results across three sections of the road. Before the merging section, the SEMI remains stable across different α values, indicating that the TTC is generally high or undefined and efficiency is dominant. Here, SEMI increases monotonically with penetration of AV, from 0.7257 to 0.8239 (for $\alpha = 1$), representing a 13.5% increase, and up to 16.6% with $\alpha = 0.6$.

However, after merging, the SEMI is more sensitive to α. As α decreases, the SEMI values drop significantly, revealing that safety becomes more influential in this section. For example, SEMI increases from 0.6917 to 0.8424 across AV rates with $\alpha = 0.9$, and from 0.5862

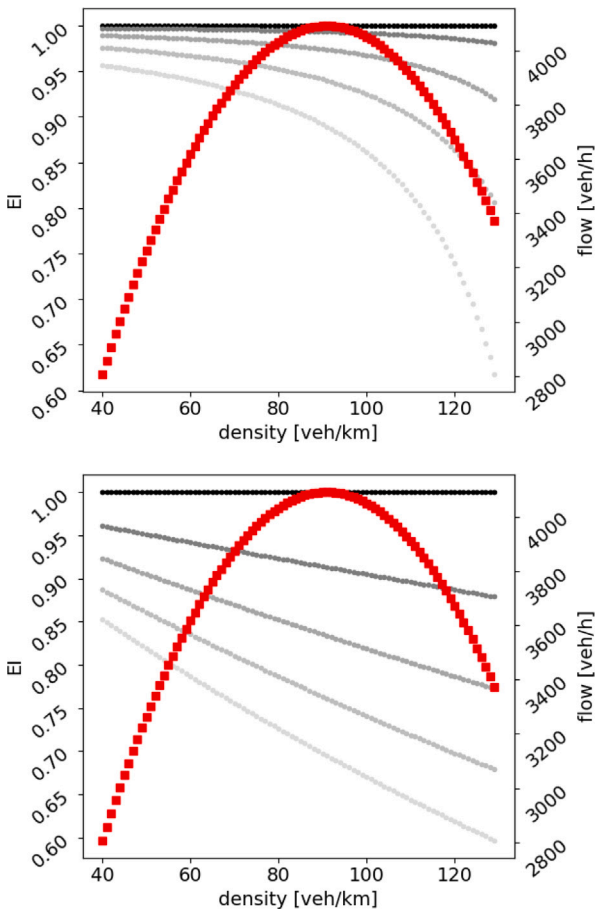

Fig. 10. Comparison of EI with the fundamental diagram. Top: vehicle speeds vary from 0 m/s (black) to 4 m/s (lightest gray) in 1 m/s steps, with constant inter-vehicle distances. Bottom: inter-vehicle distances vary from 0 m (black) to 8 m (lightest gray) in 2 m steps, with constant speeds.

Table 5
Mean of total SEI values during rush hours for different penetration rates of AVs.

% of AVs	Main road before merging section	Main road after merging section	On ramp
0	0.7257	0.7255	0.5144
10	0.7242	0.7221	0.4965
20	0.7280	0.7254	0.4965
30	0.7339	0.7328	0.5118
40	0.7393	0.7412	0.5161
50	0.7484	0.7561	0.5215
60	0.7584	0.7705	0.5436
70	0.7720	0.7884	0.5497
80	0.7882	0.8080	0.6495
90	0.8070	0.8340	0.5552
100	0.8239	0.8695	0.5621

to 0.7479 with $\alpha = 0.6$, which gives an improvement of 27.6%. This confirms that a higher presence of AVs improves both efficiency and safety where safety constraints are more critical.

On the on-ramp, the SEMI values also decrease with lower α, but the trend across AV rates is less monotonic for low penetration levels. Overall, SEMI still improves with increasing AV penetration, though to a lesser extent and with more variability due to the complex and transitional nature of ramp traffic.

5. Discussion

The proposed Efficiency Index (EI) and Safety and Efficiency Index (SEI) provide a compact but informative framework to evaluate traffic performance based on microscopic data. EI captures how vehicles move harmoniously, rewarding uniform speed and consistent spacing, while SEI adds a safety dimension based on time-to-collision (TTC). To address cases where efficiency can mask unsafe behavior, we introduce the SEMI, which includes a tunable penalty factor $\alpha \in (0, 1]$ to place greater emphasis on safety. These indicators are designed to cover common maneuvers such as car-following, lane changes, and emergency braking. Although merging scenarios are not explicitly modeled yet, the formulation is adaptable. We tested the indicators using real traffic data from the city of Gothenburg in microsimulations that include mixed traffic and varying penetration rates of autonomous vehicles (AVs). The results showed that EI and SEI increased by up to 13.5% on a main road section before merging and up to 19.8% after merging during peak hours as penetration of AV increased. In the section before merging, where traffic flow was lower, SEMI was insensitive to changes in α, suggesting that efficiency was dominant. In contrast, SEMI values decreased significantly post-merging with decreasing α, indicating a stronger influence of safety. As vehicle-level data become more widely available through connected and autonomous systems, these indicators could support practical applications such as individual vehicle path planning and real-time traffic management (e.g., dynamic speed limits or rerouting). In broader research contexts, they offer a valuable

Table 6
Mean of total SEMI values during rush hours for different penetration rates of AVs and different values of α on the main road before merging section.

% of AVs	$\alpha = 0.9$	$\alpha = 0.8$	$\alpha = 0.7$	$\alpha = 0.6$
0	0.7256	0.7254	0.7253	0.7250
10	0.7240	0.7237	0.7247	0.7236
20	0.7265	0.7263	0.7275	0.7260
30	0.7331	0.7343	0.7321	0.7320
40	0.7391	0.7389	0.7380	0.7379
50	0.7483	0.7481	0.7480	0.7479
60	0.7584	0.7584	0.7584	0.7582
70	0.7719	0.7715	0.7710	0.7709
80	0.7870	0.7847	0.7841	0.7840
90	0.8045	0.8059	0.8048	0.8038
100	0.8239	0.8238	0.8238	0.8237

Table 7
Mean of total SEMI values during rush hours for different penetration rates of AVs and different values of α on the main road after merging section.

% of AVs	$\alpha = 0.9$	$\alpha = 0.8$	$\alpha = 0.7$	$\alpha = 0.6$
0	0.6917	0.6558	0.6201	0.5862
10	0.6893	0.6569	0.6246	0.5896
20	0.6963	0.6630	0.6339	0.6004
30	0.7028	0.6733	0.6421	0.6105
40	0.7122	0.6818	0.6555	0.6250
50	0.7245	0.7965	0.6691	0.6401
60	0.7406	0.7111	0.6830	0.6519
70	0.7578	0.7288	0.7004	0.6714
80	0.7781	0.7482	0.7213	0.6924
90	0.8049	0.7756	0.7463	0.7181
100	0.8424	0.8098	0.7793	0.7479

Table 8
Mean of total SEMI values during rush hours for different penetration rates of AVs and different values of α on ramp.

% of AVs	$\alpha = 0.9$	$\alpha = 0.8$	$\alpha = 0.7$	$\alpha = 0.6$
0	0.4670	0.4379	0.3859	0.3416
10	0.4526	0.4271	0.3643	0.3430
20	0.4899	0.4316	0.3832	0.3368
30	0.4886	0.4356	0.3894	0.3304
40	0.4736	0.4544	0.4114	0.3383
50	0.5075	0.4568	0.4100	0.3659
60	0.5120	0.4665	0.4243	0.3806
70	0.5172	0.4810	0.4280	0.3695
80	0.5360	0.4910	0.4244	0.3816
90	0.5517	0.4784	0.4507	0.3903
100	0.5685	0.4987	0.4536	0.3917

tool for evaluating the implications of AV behavior models, vehicle cooperation strategies, or infrastructure changes. However, the current validation of the indicators is limited to motorway-like scenarios using SUMO. Future research should explore their applicability in more complex environments such as intersections, roundabouts, or areas with vulnerable road users. Additionally, while TTC is a standard surrogate safety measure, alternative indicators such as Time to React (TTR) or Modified TTC (MTTC) could be explored to enhance robustness. Finally, establishing operational thresholds for safety and efficiency, such as when stop-and-go patterns occur, could support absolute, rather than just comparative, evaluations.

6. Conclusion

This study presents three new indicators – EI, SEI, and SEMI – to evaluate traffic efficiency and safety at the microscopic level. Their flexibility and reliance on vehicle-level quantities make them especially relevant in the era of AVs and connected mobility. Beyond simulation, their interpretability enables use in planning, behavior modeling, and traffic control systems. For policy and planning, these indicators offer a practical way to assess trade-offs between safety and efficiency, which are often treated separately. By integrating these two aspects, our framework provides a more holistic perspective that can be applied to support AV deployment strategies, infrastructure planning, and traffic management interventions. The interdisciplinary relevance of the proposed indicators lies in their potential applications in transport engineering, data science, behavioral modeling, and public policy, for example, the indicators can be used by urban planners to assess infrastructure impacts, by system designers to calibrate AV behavior, or by traffic psychologists studying driver responses in mixed environments. Future work will focus on extending these indicators to urban settings and refining their formulations for broader safety metrics and use cases. Continued interdisciplinary collaboration will be essential to ensure their robustness, acceptance, and integration into real-world traffic systems.

CRediT authorship contribution statement

Eleonora Andreotti: Writing – review & editing, Writing – original draft, Visualization, Software, Methodology, Formal analysis, Conceptualization. **Selpi:** Writing – review & editing, Supervision, Funding acquisition.

Declaration of competing interest

The authors declare the following financial interests/personal relationships which may be considered as potential competing interests: Eleonora Andreotti reports financial support was provided by Swedish Innovation Agency Vinnova. Selpi reports financial support was provided by Swedish Innovation Agency Vinnova. Eleonora Andreotti reports financial support was provided by Chalmers Area of Advance Transport for DS- Auto. Selpi reports financial support was provided by Chalmers Area of Advance Transport for DS- Auto. If there are other authors, they declare that they have no known competing financial interests or personal relationships that could have appeared to influence the work reported in this paper.

Acknowledgments

This work is financially supported by Sweden's Innovation Agency Vinnova, grant no. 2018-02891 and Chalmers Area of Advance Transport for DS-Auto.

Data availability

Microscopic traffic data used for simulation are based on publicly available traffic flow records from the Swedish Transport Administration (Trafikverket) for 8-9 April 2019.

References

Allen, B.L., Shin, B.T., Cooper, P.J., 1978. Analysis of traffic conflicts and collisions. Transp. Res. Rec. (667), 67–74.

Andreotti, E., Boyraz, P., Selpi, 2020. Safety-centred analysis of transition stages to traffic with fully autonomous vehicles. In: IEEE Int. Conf. on Intelligent Transportation Systems, Rhodes, Greece, 2020. In: ITSC2020, pp. 1–6. http://dx.doi.org/10.1109/ITSC45102.2020.9294644.

Andreotti, E., Selpi, Aramrattana, M., 2022a. Cooperative merging strategy between connected autonomous vehicles in mixed traffic. IEEE Open J. Intell. Transp. Syst. 3, 825–837. http://dx.doi.org/10.1109/OJITS.2022.3179125.

Andreotti, E., Selpi, Boyraz, P., 2022b. Potential impact of autonomous vehicles in mixed traffic from simulation using real traffic flow. J. Intell. Connect. Veh..

Aramrattana, M., Larsson, T., Englund, C., Jansson, J., Nåbo, A., 2020. A novel risk indicator for Cut-In situations. In: IEEE Int. Conf. on Intelligent Transportation Systems, Rhodes, Greece, 2020. In: ITSC2020, pp. 1–6. http://dx.doi.org/10.1109/ITSC45102.2020.9294315.

Arvin, R., Khattak, A.J., Kamrani, M., Rio-Torres, J., 2021. Safety evaluation of connected and automated vehicles in mixed traffic with conventional vehicles at intersections. J. Intell. Transp. Syst. 25 (2), 170–187. http://dx.doi.org/10.1080/15472450.2020.1834392.

Bjørnskau, T., Waersted, H., Christensen, P., Philips, I., 2023. "Game over" for autonomous shuttles in mixed traffic? Lessons from a real-world pilot in Oslo, Norway. Transp. Res. Interdiscip. Perspect. 28, 100631. http://dx.doi.org/10.1016/j.trip.2023.100631.

Brilon, W., 2000. Traffic flow analysis beyond traditional methods. Transp. Res. Circ. 26–41.

Cooper, P., 1984. Experience with traffic conflicts in Canada with emphasis on "Post Encroachment Time" techniques. In: Asmussen, E. (Ed.), International Calibration Study of Traffic Conflict Techniques. In: NATO ASI Series (Series F: Computer and Systems Sciences), Vol. 5, Springer, Berlin, Heidelberg, pp. 75–96.

Daganzo, C.F., Gayah, V.V., Gonzales, E.J., 2011. Macroscopic relations of urban traffic variables: Bifurcations, multivaluedness and instability. Transp. Res. B: Methodol. 45 (1), 278–288.

Daganzo, C.F., Geroliminis, N., 2008. An analytical approximation for the macroscopic fundamental diagram of urban traffic. Transp. Res. B: Methodol. 42 (9), 771–781. http://dx.doi.org/10.1016/j.trb.2008.06.008.

Erlandson, W., 2020. Traffic Flow Implications of Driverless Trucks. Microscopic traffic simulations using SUMO (Master's thesis). Lund University, Lund, Sweden.

Frantzeskakis, J.M., Iordanis, D.I., 1987. Volume-to-capacity ratio and traffic accidents on interurban four-lane highways in Greece. Transp. Res. Rec. 1112, 29–38.

Greenshields, B.D., 1935. A study of traffic capacity. In: Proceedings of the Highway Research Board. 14, pp. 448–477.

Guériau, M., Dusparic, I., 2020. Quantifying the impact of connected and autonomous vehicles on traffic efficiency and safety in mixed traffic. In: 2020 IEEE 23rd International Conference on Intelligent Transportation Systems (ITSC). pp. 1–8. http://dx.doi.org/10.1109/ITSC45102.2020.9294174.

Guido, G., Saccomanno, F., Vitale, A., Astarita, V., Festa, D.C., 2011. Comparing safety performance measures obtained from video capture data. J. Transp. Eng.- Asce 137, 481–491.

He, F., Yan, X., Liu, Y., Ma, L., 2016. A traffic congestion assessment method for urban road networks based on speed performance index. Procedia Eng. 137, 425–433. http://dx.doi.org/10.1016/j.proeng.2016.01.277, Green Intelligent Transportation System and Safety.

Hu, L., Ou, J., Huang, J., Chen, Y., Cao, D., 2020. A review of research on traffic conflicts based on intelligent vehicles. IEEE Access 8, 24471–24483. http://dx.doi.org/10.1109/ACCESS.2020.2970164.

Imran, M., et al., 2024. Macroscopic modeling of connected, autonomous and human-driven vehicles: A pragmatic perspective. Transp. Res. Interdiscip. Perspect. 100735, http://dx.doi.org/10.1016/j.trip.2024.100735.

Kato, H., Sanko, N., Masashi, 2023. Value of travel time savings for leisure trip in autonomous vehicles: Case study from the Tokyo Metropolitan Area. Transp. Res. Interdiscip. Perspect. 24, 100xxx. http://dx.doi.org/10.1016/j.trip.2023.xxx.

Kesting, A., Treiber, M., Helbing, D., 2010. Enhanced intelligent driver model to access the impact of driving strategies on traffic capacity. Philos. Trans. Ser. A Math. Phys. Eng. Sci. 368 (1928), 4585—4605. http://dx.doi.org/10.1098/rsta.2010.0084.

Knoop, V.L., Hoogendoorn, S.P., Shiomi, Y., Buisson, C., 2012. Quantifying the number of lane changes in traffic: Empirical analysis. Transp. Res. Rec. 2278 (1), 31–41. http://dx.doi.org/10.3141/2278-04, arXiv:https://doi.org/10.3141/2278-04.

Krajzewicz, D., Erdmann, J., Behrisch, M., Bieker, L., 2012. Recent development and applications of SUMO - Simulation of Urban MObility. Int. J. Adv. Syst. Meas. 5 (3&4), 128–138.

Li, Z., Chitturi, M.V., Zheng, D., Bill, A.R., Noyce, D.A., 2013. Modeling reservation-based autonomous intersection control in VISSIM. Transp. Res. Rec. 2381 (1), 81–90. http://dx.doi.org/10.3141/2381-10.

Li, G., Li, S.E., Jia, L., Wang, W., Cheng, B., Chen, F., 2015. Driving maneuvers analysis using naturalistic highway driving data. In: 2015 IEEE 18th International Conference on Intelligent Transportation Systems. pp. 1761–1766. http://dx.doi.org/10.1109/ITSC.2015.286.

Lu, W., Liu, J., Mao, J., Hu, G., Gao, C., Liu, L., 2020. Macroscopic fundamental diagram approach to evaluating the performance of regional traffic controls. Transp. Res. Rec. 2674 (7), 420–430. http://dx.doi.org/10.1177/0361198120923359.

Luo, L., Liu, Y., Feng, Y., Liu, H.X., Ge, Y.-E., 2024. Stabilizing traffic flow by autonomous vehicles: Stability analysis and implementation considerations. Transp. Res. C: Emerg. Technol. 158, 104449. http://dx.doi.org/10.1016/j.trc.2023.104449.

Mahdavian, A., Shojaei, A., Oloufa, A., 2019. Assessing the Long- and Mid-Term effects of connected and automated vehicles on highways' traffic flow and capacity. In: International Conference on Sustainable Infrastructure 2019. ASCE, pp. 263–273. http://dx.doi.org/10.1061/9780784482650.027.

Mahmud, S.S., Ferreira, L., Hoque, M.S., Tavassoli, A., 2017. Application of proximal surrogate indicators for safety evaluation: A review of recent developments and research needs. IATSS Res. 41 (4), 153–163. http://dx.doi.org/10.1016/j.iatssr.2017.02.001.

Mamdoohi, A., Zavareh, M., Hydén, C., Nordjaern, T., 2014. Comparative analysis of safety performance indicators based on inductive loop detector data. Promet - Traffic - Traffico 26 (2), 139–149. http://dx.doi.org/10.7307/ptt.v26i2.1273.

Meng, Q., Qu, X., 2012. Estimation of rear-end vehicle crash frequencies in urban road tunnels. Accid. Anal. Prev. 48, 254–263.

Michael, P.G., Leeming, F.C., Dwyer, W.O., 2000. Headway on urban streets: observational data and an intervention to decrease tailgating. Transp. Res. F: Traffic Psychol. Behav. 3 (2), 55–64. http://dx.doi.org/10.1016/S1369-8478(00)00015-2.

Minderhoud, M.M., Bovy, P.H., 2001. Extended time-to-collision measures for road traffic safety assessment. Accid. Anal. Prev. 33 (1), 89–97. http://dx.doi.org/10.1016/S0001-4575(00)00019-1.

Morando, M.M., Tian, Q., Truong, L., Vu, H.L., 2018. Studying the safety impact of autonomous vehicles using simulation-based surrogate safety measures. J. Adv. Transp. 2018, 6135183.

Nilsson, F., 2019. Simulation-based Analysis of Partially Automated Vehicular Networks. A Parametric Analysis Utilizing Traffic Simulation (Master's thesis). Chalmers University of Technology, Gothenburg, Sweden.

Othayoth, D., Rao, K.K., 2020. Investigating the relation between level of service and Volume-to-Capacity ratio at signalized intersections under heterogeneous traffic condition. Transp. Res. Procedia 48, 2929–2944. http://dx.doi.org/10.1016/j.trpro.2020.08.190, Recent Advances and Emerging Issues in Transport Research – An Editorial Note for the Selected Proceedings of WCTR 2019 Mumbai.

Ozbay, K., Yang, H., Bartin, B., Mudigonda, S., 2008. Derivation and validation of new simulation-based surrogate safety measure. Transp. Res. Rec. 2083 (1), 105–113. http://dx.doi.org/10.3141/2083-12.

Park, J.E., Byun, W., Kim, Y., Ahn, H., Shin, D.K., 2021. The impact of automated vehicles on traffic flow and road capacity on urban road networks. J. Adv. Transp. 2021, 10. http://dx.doi.org/10.1155/2021/8404951.

Parsa, A.B., Shabanpour, R., Mohammadian, A.K., Auld, J., Stephens, T., 2020. A data-driven approach to characterize the impact of connected and autonomous vehicles on traffic flow. Transp. Lett. 1–9. http://dx.doi.org/10.1080/19427867.2020.1776956.

Pipes, L.A., 1967. Car following models and the fundamental diagram of road traffic. Transp. Res. 1, 21–29.

Sala, M., Soriguera, F., 2021. Capacity of a freeway lane with platoons of autonomous vehicles mixed with regular traffic. Transp. Res. B: Methodol. 147, 116–131. http://dx.doi.org/10.1016/j.trb.2021.03.010.

Sánchez, N.C., Larson, K., 2024. Shared autonomous micro-mobility for walkable cities. Transp. Res. Interdiscip. Perspect. 27, 101236. http://dx.doi.org/10.1016/j.trip.2024.101236.

Silva, Ó., Cordera, R., González-González, E., Nogués, S., 2022. Environmental impacts of autonomous vehicles: A review of the scientific literature. Sci. Total Environ. 830, 154615.

Singh, S., 2015. Critical reasons for crashes investigated in the national motor vehicle crash causation survey. In: Traffic Safety Facts Crash Stats National Highway Traffic Safety Administration. pp. 1–2.

2019. Trafikverket. Accessed 17 September 2020.

Virdi, N., Grzybowska, H., Waller, S.T., Dixit, V., 2019. A safety assessment of mixed fleets with connected and autonomous vehicles using the surrogate safety assessment module. Accid. Anal. Prev. 131, 95–111.

Vogel, K., 2003. A comparison of headway and time to collision as safety indicators. Accid. Anal. Prev. 35 (3), 427–433. http://dx.doi.org/10.1016/S0001-4575(02)00022-2.

Wang, C., Xie, Y., Huang, H., Liu, P., 2021. A review of surrogate safety measures and their applications in connected and automated vehicles safety modeling. Accid. Anal. Prev. 157, 106157. http://dx.doi.org/10.1016/j.aap.2021.106157.

Wardrop, J., 1952. Road paper. some theoretical aspects of road traffic research. In: Proceedings of the Institute of Civil Engineers, Part II. Vol. I, pp. 325–378, No. 2.